■ 631

Matrix Mask Overlapping and Convolution Eight Directions for Blood Vessel Segmentation on Fundus Retinal Image

Arif Muntasa*, Indah Agustien Sirajudin, Mochammad Kautsar Sophan
Informatics Engineering Department, Enginering Faculty, University of Trunojoyo
Ry Telang Po. Box 2 Kamal, Bangkalan
*Corresponding author, e-mail: arifmuntasa@if.trunojoyo.ac.id

Abstract

Diabetic Retinopathy is one of the diseases that have the effect of a high mortality rate after heart disease and cancer. However, the disease can be early detected through blood vessels and the optic nerve head in Fundus images. Blood vessels separation of the optic nerve head required high effort when it is conducted manually, therefore it is necessary that the appropriate method to perform segmentation of the object. Level Set method is well-known as object segmentation method based on object deformable. However, the methods have the disadvantage; it requires initialization before the segmentation process. In this research, segmentation method without initialization process is proposed. The segmentation is conducted by using the maximum value selection results of convolution 8 directions. Experimental results show that, proposed method has obtained 89.48% accuracy. Segmentation errors are caused by small branches, where they are not connected, so that the objects are supposed as noises.

Keywords: fundus image, segmentation, 8 directions convolution, overlapping

1. Introduction

One of diabetic retinopathy indications is eyes retinal defect. Hard defect will cause blindness [1]-[4], therefore, it is necessary to be conducted early detection on Fundus. In this case, segmentation of blood vessel in Fundus plays important rule in detecting eye blood vessel damage [5]. The segmentation results such as length, wide, shape of blood vessel branch will assist to determine kind of the diabetic retinopathy diseases [6]. The problem occurred on medical world related to blood vessel on Fundus is difficult to segment manually blood vessel, it is require high cost and accuracy. However, blood vessel segmentation is not professional if it is conducted manually [7].

Difficulty segmentation on the Fundus image blood vessels caused by optic nerve head damage has gray level that is almost similar to the objects around and overlapping between the blood vessels and the optic nerve head. Therefore it is necessary to build appropriate method for blood vessels segmentation in the Fundus image.

In recent years, many researchers have conducted research on the segmentation of the blood vessels of the Fundus [7]-[10], Optic Nerve Head [11]-[14]. The research conducted is an attempt to improve the segmentation result Fundus image blood vessels. However, the results of segmentation error rate are still far from the expected.

The method is widely used to detect blood vessels is Level Set [14], but the method has a limitation when the segmentation process which requires appropriate initialization region, if it does not match actual outcomes result in high error rates. In this study, the proposed segmentation method without using a Fundus blood vessel region initialization, the proposed method based on the maximum value of the convolution matrix 8 directions and overlapping mask matrix. The proposed method works quickly.

Segmentation of blood vessels and the determination of the optic disc is a series of Fundus image biomedical research process used to detect levels of diabetic disease retinopathy [15]. Object separation Fundus image blood vessels are very complicated process. The problem that arises when the segmentation process is very little difference between the blood vessels and other objects that are around, it will cause difficulty in performing segmentation. The number of pixels on the blood vessels and the optic disc overlapping also cause difficulty in performing segmentation. However, many methods have been developed by the researcher to

segment the blood vessels and the optic disc on Fundus image. The presence of cotton wools spots, microanuerysms, edema and exudates are also an impediment to separate the blood vessels and the optic nerve disc.

2. Research Method

Fundus image has black background, whereas blood vessel and optic disk have the little difference to the background. This problem causes difficulty to separate between the blood vessel and the background. In this research, the proposed method Fundus blood vessel segmentation by determining the maximum value of the convolution matrix followed by an 8-directions overlapping mask matrix. Suppose an RGB fundus image as in the form of the following equation

$$F_{RGB} = \begin{pmatrix} f_{rgb}(1,1) & f_{rgb}(1,2) & \cdots & f_{rgb}(1,w) \\ f_{rgb}(2,1) & f_{rgb}(2,2) & \cdots & f_{rgb}(2,w) \\ \vdots & \vdots & \ddots & \vdots \\ f_{rgb}(h,1) & f_{rgb}(h,2) & \cdots & f_{rgb}(h,w) \end{pmatrix} \quad (1)$$

For the next process, green value of the Equation (1) is processed as seen on the following equation

$$F_G = \begin{pmatrix} f_g(1,1) & f_g(1,2) & \cdots & f_g(1,w) \\ f_g(2,1) & f_g(2,2) & \cdots & f_g(2,w) \\ \vdots & \vdots & \ddots & \vdots \\ f_g(h,1) & f_g(h,2) & \cdots & f_g(h,w) \end{pmatrix} \quad (2)$$

In order to create mask image, it is necessary to determine the threshold value. It is conducted to separate between Fundus object and background. The following are equation to create the mask image using the threshold value

$$Mask = \begin{cases} 0 & if & F_G < threshold \\ 255 & else \end{cases} \quad (3)$$

Mask image can be created from Equation (2) by using Equation (3) as seen in Figure 1. In this case, the threshold value used is 50.
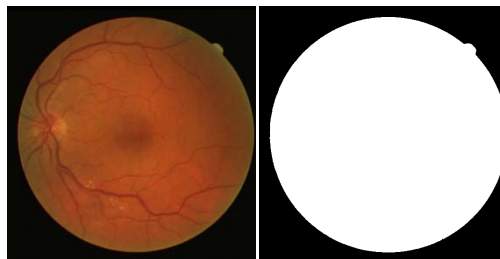

Figure 1. Fundus Image DRIVE Database and Mask Image

The next step is to calculate the result of the convolution matrix 8 directions. This process is started by defining the integer number x and $x \in \{-t, -5, -4, \ldots, 4, 5\}$. The value of x is computed by using equation

$$Y = -\frac{x.*x}{2\sigma^2} \tag{4}$$

The results of Equation (4) are shifted the value based on the maximum value as seen on the following equation

$$V = \max(Y) - Y \tag{5}$$

The results of Equation (5) are duplicated n lines and calculated the average values by using equation

$$U = \frac{1}{MN} \sum_{j=1}^{n} \sum_{k=1}^{m} V_{j,k} \tag{6}$$

Zero means value can be calculated based on Equation (5) and (6) as the following equation

$$Z = V - U \tag{7}$$

The results of Equation (7) are normalized by using equation

$$R = \frac{Z_{h,w}}{\sum_{n=1}^{h} \sum_{m=1}^{w} Z_{n,m}} \tag{8}$$

In this case, the 1st row of R has the same value with the 2nd row until the end row. The value of R can be seen in equation

$$R = \begin{pmatrix} R_{1,1} & R_{1,2} & \cdots & R_{1,t} \\ R_{2,1} & R_{2,2} & \cdots & R_{2,t} \\ \vdots & \vdots & \ddots & \vdots \\ R_{t-4,1} & R_{t-4,2} & \cdots & R_{t-4,t} \end{pmatrix} \tag{9}$$

The results of Equation (9) is used to created mask matrix by using the following rule as seen on the following equation

$$R = \begin{pmatrix} 0 & 0 & 0 & 0 & 0 & 0 \\ 0 & 0 & 0 & 0 & 0 & 0 \\ 0 & 0 & 0 & 0 & 0 & 0 \\ 0 & R_{1,1} & R_{1,2} & \cdots & R_{1,t} & 0 \\ 0 & R_{2,1} & R_{2,2} & \cdots & R_{2,t} & 0 \\ \vdots & \vdots & \vdots & & \vdots & \vdots \\ 0 & R_{t-4,1} & R_{t-4,2} & \cdots & R_{t-4,t} & 0 \\ 0 & 0 & 0 & 0 & 0 & 0 \\ 0 & 0 & 0 & 0 & 0 & 0 \\ 0 & 0 & 0 & 0 & 0 & 0 \end{pmatrix} \tag{10}$$

Mask matrix in Equation (10) is rotated by using angles 20^0 until 160^0 (M_{20}^0, M_{40}^0, M_{60}^0, M_{80}^0, M_{100}^0, M_{120}^0, M_{140}^0, and M_{160}^0)

$$Q_j = F_G \otimes M_j, j \in 20^0, 40^0, \ldots \ldots 160^0 \tag{11}$$

The result of the convolution of Equation (11) is checked every pixel, the largest value will be taken and placed on the position of the corresponding pixel

$$R = \max(Q_j) \tag{12}$$

The results of selecting the maximum value of the convolution is taken the most minimal value and normalized by using equation

$$S = \min(R) \tag{13}$$

$$H = (R + S) * \frac{255}{\max(\max(R + S))} \tag{14}$$

Value of the matrix H is the screening results of convolution matrix 8 directions. Furthermore, the results of Equation (14) is used to determine the threshold value of the image by comparing sum of the largest value by using equation

$$T = \max(T1_i + T2_i) \tag{15}$$

$$T1_i = -\frac{1}{2} * \sum_{n=1}^{i} H_{n,m} * \log 2 * \left(\sum_{n=1}^{i} H_{n,m} + \alpha \right)$$

and $\qquad\qquad\qquad\qquad\qquad\qquad\qquad\qquad\qquad\qquad\qquad$ (16)

$$T2_i = -\frac{1}{2} * \sum_{n=i+1}^{256} H_{n,m} * \log 2 * \left(\sum_{n=i+1}^{256} H_{n,m} + \alpha \right)$$

The results of Equation (16) are used to change Fundus object, but background image is not changed as seen on the following equation

$$B = \begin{cases} 0 & if \quad H \geq T \quad and \quad Mask = 255 \\ 1 & else \end{cases} \tag{17}$$

Binary image results in Equation (17) are also contain some noises, therefore it is necessary to remove the breadth of its noise is less than the threshold value. Objects that are smaller than the threshold value is changed to black as the following equation

$$E = \begin{cases} 0 & if \quad O_i \leq ObjThreshold \\ 1 & else \end{cases} \tag{18}$$

The results of equation (19) is then overlapped with mask image of Equation (3) by using the following equation

$$Seg =\sim \left(\sim E + \sim Mask \right) \tag{19}$$

Accuracy Measurements of Segmentation Results
    To obtain accuracy the segmentation results on Fundus image DRIVE database [16], it is necessary to be calculated the difference between experimental results and ground truth image database by using *Miss Classification Error* equation

$$ME = 1 - \frac{\left(Seg_{BG} \cap Seg_{BT} \right) + \left(Seg_{FG} \cap Seg_{FT} \right)}{\left| Seg_{BG} \right| + \left| Seg_{BT} \right|} \tag{20}$$

In this case Seg_{BG} and Seg_{BT} represent background and foreground ground truth images, whereas background and foreground ground truth images of segmentation results are represented by using Seg_{FG} and Seg_{FT}.

3. Results and Analysis
    To prove performance of the proposed method, the DRIVE Fundus image database is used for experiments [16]. It consists of 20 images. It also supported the segmentation results, the segmentation results are performed by people who are experts in related fields. In order to obtain segmentation accuracy, experimental results are compared with ground truth Fundus image DRIVE database. The following are examples of Fundus image DRIVE database.
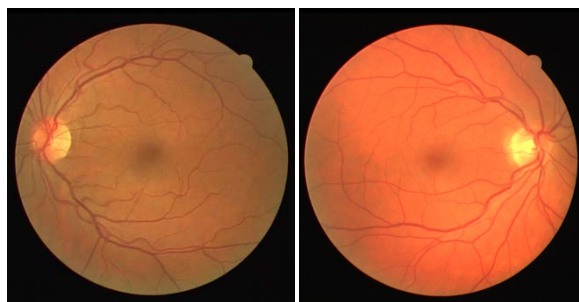

Figure 2. Two Fundus Images on DRIVE Database [16]

The ground truth Fundus image DRIVE databases can be seen Figure 3 and Figure 4. Fundus image DRIVE databases have two ground truth models, which are the first model (Figure 3) and the second model (Figure 4).
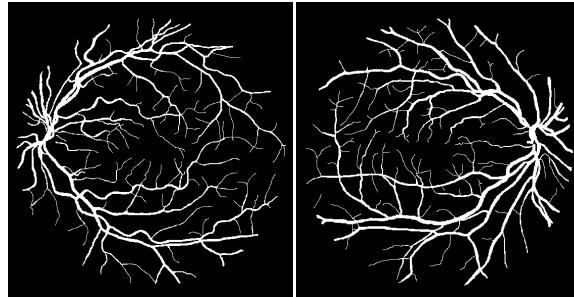
Figure 3. The First Model Ground Truth DRIVE Database [16]

Figure 4. The Second Model Ground Truth DRIVE Database [16]

The experimental results have been compared with the first ground truth model of Fundus DRIVE images database. The experimental results of proposed method show that the minimum accuracy is 62.28%, the average of segmentation accuracy is 89.48%, and the maximum segmentation accuracy is 99.744 as shown in Figure 5.
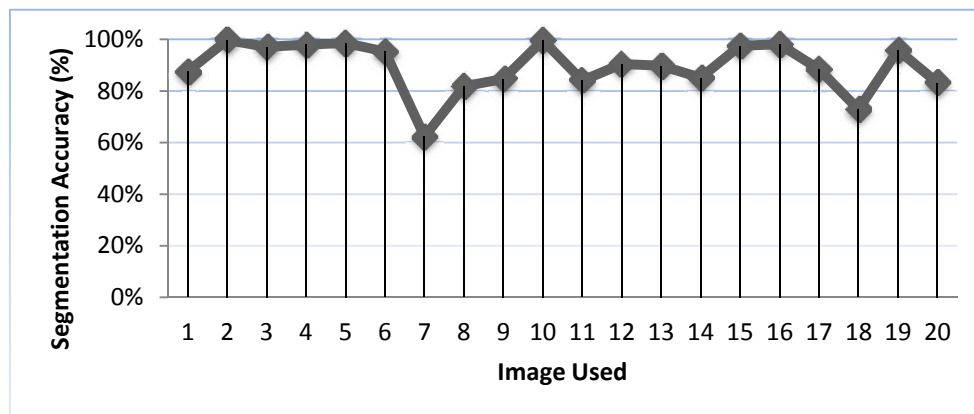

Figure 5. The Segmentation Accuracy of Proposed Method on Fundus DRIVE images database

The biggest error occurs on the 7th image. Error on image is influenced by some parameters, which are the threshold values of object is deleted, wide object, round of object, and ratio between the area of circumference of object. The presence of blood vessels of branch object is regarded as noise, but the elongated shape of the object apart from its branches so it would be deleted when the deletion is conducted. The following are the segmentation results of proposed method as seen on Figure 6.
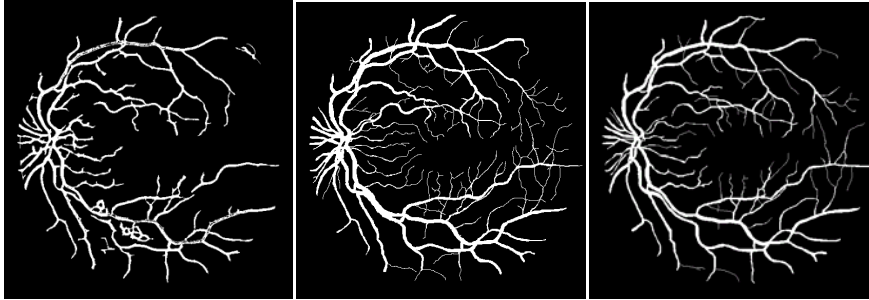
Figure 6. The segmentation results, the 1st and the 2nd Ground Truth (from the left to the right)

The difference between background and blood vessels has resulted in breaking of the ends of the retinal blood vessels. Separation between the ends of the retinal blood vessels and the main branch has formed small objects. The object is regarded as noise and removed along with the actual noise as shown in Figure 7. Both for parts A and B of Figure 7 are the pieces of the retinal image have been enlarged to 400%. Part A of Figure 7 shows that there is a separate ends of the blood vessels of the main branch. Part B of Figure 7 describes of the ends of the severed blood vessels is regarded as noise and removed at the time of the actual noise removal process. The error resulted in sensitivity and accuracy values decreased.
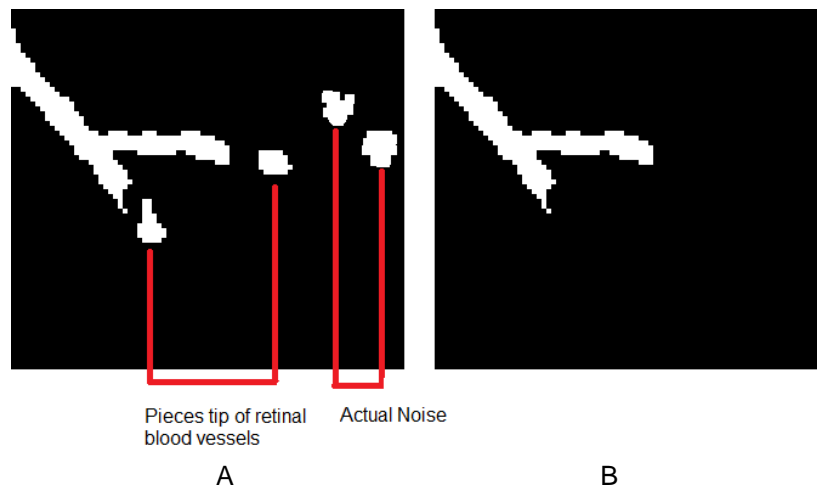

Figure 7. Explanation of Image Segmentation Fault
A. Ends of the retinal blood vessels that is separate from the main branch.
B. Pieces tip of retinal blood vessels has been removed because it is considered as noise

Our proposed method has been compared to other method as seen In Table 1. The compariason result shows that our proposed method is superior to the other two methods. However, it is important to improve our proposed method to increase the accuracy. Common errors that occur in each object is caused by two things. The first error, delicate branches of blood vessels can not be detected, because the delicate branches of blood vessels has been cut off from the main branch and the branch is considered as noise. The second error, excessive dilation process that causes blood vessel branches is formed too thick.

Table 1. Comparison of the segmentation results Accuracy

Method	Accuracy (%)
Chaudhuri et al. [17]	87.77
Jiang et al. [18]	89.11
Our Proposed Method	89.48

4. Conclusion

The proposed method has been able to segment the Fundus image DRIVE database, the average error rate 10.52%. However, the error that occurs in some Fundus image can be improved by considering several parameters, especially the determination of the threshold of widespread objects that are considered noise. The determination of the object threshold value needs to be carried out automatically with the object labeling Fundus image segmentation results. The ratio of the circumference and area of the object is an important parameter that should be added to avoid deletion of objects that are not noise but are considered as noise.

References

[1]   Akara Sopharak, Bunyarit Uyyanonvara, Sarah Barman. "Automatic Microaneurysm Detection from Non-dilated Diabetic Retinopathy Retinal Images Using Mathematical Morphology Methods. *IAENG International Journal of Computer Science*. 2011; 38(3): 295-301.
[2]   Bock R, Meier J, Nyúl LG, Hornegger J, Michelson G. Glaucoma Risk Index: Automated Glaucoma Detection From Color Fundus. *Medical Image Analysis*. 2010; 14(3): 471-481.
[3]   Akara Sopharak, Khine Thet Nwe, Yin Aye Moe, Matthew N. Dailey, Bunyarit Uyyanonvara. *Automatic Exudate Detection with a Naive Bayes Classifier.* The 2008 International Conference on Embedded Systems and Intelligent Technology, Bangkok, Thailand. 2008.
[4]   Riveron EF., Guimeras NG. Extraction of blood vessels in ophthalmic color images of human retinas. *Lecture Notes in Computer Science.* 2006; 4225: 118–126.
[5]   Rawi MA., Qutaishat M., Arrar M. An improved matched filter for blood vessel detection of digital retinal images. *Computers in Biology and Medicine.* 2007;37(2): 262–267.
[6]   Chanwimaluang T., Fan G. *An efficient blood vessel detection algorithm for retinal images using local entropy Thresholding.* Proceedings of IEEE International Symposium on Circuits and Systems, Bangkok, Thailand. 2003; 5: 21–24.
[7]   Yong Yang, Shuying Huang, Nini Rao. An Automatic Hybrid Method For Retinal Blood Vessel Extraction. *International Journal of Application Mathetamatics and Computer Science.* 2008; 18(3): 399–407.
[8]   Staal, MD. Abr`amoff, M. Niemeijer, MA. Viergever, B. van Ginneken. Ridge based vessel segmentation in color images of the retina. *IEEE Transactions on Medical Imaging.* 2004; 23(4): 501–509.
[9]   Niemeijer, Staal, B. van Ginneken, M. Loog, MD. Abr`amoff. Comparative study of retinal vessel segmentation methods on a new publicly available database. in *SPIE Medical Imaging*, J. M. Fitzpatrick and M. Sonka, Eds. 2004; 5370: 648–656.
[10] HF. Jelinek, RM. Cesar-Jr. Segmentation of retinal fundus vasculature in non-mydriatic camera images using wavelets. *Angiography and Plaque Imaging: Advanced Segmentation Techniques*, J. Suri and T. Laxminarayan, Eds. CRC Press. 2003: 193–224.
[11] Fengshou Yin, Jiang Liu, Sim Heng Ong, Ying Sun, Damon WK. Wong, Ngan Meng Tan, Carol Cheung, Mani Baskaran, Tin Aung, Tien Yin Wong. *Model-based Optic Nerve Head Segmentation on Retinal Fundus Images.* 33rd Annual International Conference of the IEEE EMBS, Boston, Massachusetts USA, August 30 - September 3. 2011.
[12] Handayani Tjandrasa, Ari Wijayanti, Nanik Suciati. Optic Nerve Head Segmentation Using Hough Transform and Active Contours. *TELKOMNIKA.* 2012; 10(3): 531~536.
[13] Lalonde M, Beaulieu M, Gagnon L. Fast and robust optic disc detection using pyramidal decomposition and Hausdorff-based template matching. *IEEE Transaction Medical Imaging*, 2001; 20(11): 1193–1200.
[14] Yu H, Barriga ES, Agurto C, Echegaray S, Pattichis MS, Bauman W, Soliz P. Fast localization and segmentation of optic disk in retinal images using directional matched filtering and level sets, *IEEE Trans Inf Technol Biomed.* 2012; 16(4): 644-657.
[15] Ibaa Jamal, M. Usman Akram, Anam Tariq. Retinal Image Preprocessing: Background and Noise Segmentation. *TELKOMNIKA*, 2012; 10(3): 537~544.
[16] DRIVE. Digital Retinal Images for Vessel Extraction, Image Sciences Institute. Available on: URL: http://www.isi.uu.nl/Research/Databases/DRIVE, accesed 2011.
[17] S. Chaudhuri, S. Chatterjee, N. Katz, M. Nelson, M. Goldbaum. Detection of blood vessels in retinal images using two-dimensional matched filters. *IEEE Transactions on Medical Imaging.* 2002;8: 263.
[18] Jiang. J. Staal, MD. Abramoff, M. Niemeijer, MA. Viergever, B. van Ginneken. Ridge based vessel segmentation in color images of the retina. *IEEE Transactions on Medical Imaging,* 2004;23: 501.